We are IntechOpen, the world's leading publisher of Open Access books Built by scientists, for scientists

6,900
Open access books available

185,000
International authors and editors

200M
Downloads

Our authors are among the

154
Countries delivered to

TOP 1%
most cited scientists

12.2%
Contributors from top 500 universities



WEB OF SCIENCE™

Selection of our books indexed in the Book Citation Index in Web of Science™ Core Collection (BKCI)

Interested in publishing with us?
Contact book.department@intechopen.com

Numbers displayed above are based on latest data collected.
For more information visit www.intechopen.com



Chapter 5

Efficient Optical Modulation of Terahertz Transmission in Organic and Inorganic Semiconductor Hybrid System for Printed Terahertz Electronics and Photonics

Tatsunosuke Matsui, Keisuke Takano,
Makoto Nakajima and Masanori Hangyo

Additional information is available at the end of the chapter

http://dx.doi.org/10.5772/64033

Abstract

Highly efficient optical modulation of terahertz (THz) transmission through Si substrate coated with thin layer of organic π-conjugated materials was investigated under various laser light irradiation conditions using THz time-domain spectroscopy. As in the pioneering work by Yoo et al. [Yoo et al., Applied Physics Letters. 2013;103:151116-1–151116-3.], we also used copper phthalocyanine (CuPc). It was perceived that the charge carrier transfer from Si to CuPc is crucial for the photo-induced metallization and efficient optical modulation of THz transmission. We found that the thickness of CuPc layer is a critical parameter to realize high charge carrier density for efficient THz transmission modulation. We also fabricated a split-ring resonator (SRR) array metamaterial on CuPc-coated Si utilizing superfine inkjet printer and succeeded in obtaining efficient modulation of resonant responses of SRR array metamaterials by laser light irradiation. We have further investigated THz transmission modulation through Si substrates coated with another four solution-processable π-conjugated materials. Two of them are π-conjugated low molecules such as the [6,6]-phenyl-C61-butyric acid methyl ester (PCBM) and 6,13-bis(triisopropylsilylethynyl) pentacene (TIPS-pentacene), and another two are the π-conjugated polymer materials such as poly[5-(2-ethylhexyloxy)-2-methoxycyanoterephthalyliden] (MEH-CN-PPV) and poly(benzimidazobenzophenanthroline) (BBL). Among these four π-conjugated materials, PCBM- and TIPS-pentacene showed better modulation efficiencies even higher than CuPc. Our findings may open the way to fabricating various types of THz active devices utilizing printing technologies.

Keywords: π-conjugated material, solution process, terahertz, metamaterial, terahertz time-domain spectroscopy

INTECH
open science | open minds

© 2016 The Author(s). Licensee InTech. This chapter is distributed under the terms of the Creative Commons Attribution License (http://creativecommons.org/licenses/by/3.0), which permits unrestricted use, distribution, and reproduction in any medium, provided the original work is properly cited. CC BY

1. Introduction

Wide range of electromagnetic waves from radio waves, microwaves to infrared, visible, and ultraviolet has been widely utilized in wide variety of applications such as lightings, displays, information and communications technology (ICT), spectroscopies, and microscopes. Among these frequency ranges, terahertz (THz) frequency range has not been explored much compared to other frequency ranges. However, researches on THz science and technologies have made significant progress in recent years [1, 2]. THz frequency range lies in between microwave and infrared as schematically shown in **Figure 1** and can be utilized for various types of applications such as spectroscopy, nondestructive inspection, security, and ICT. For wider spread usage of THz technologies, development of useful optical devices is demanded.

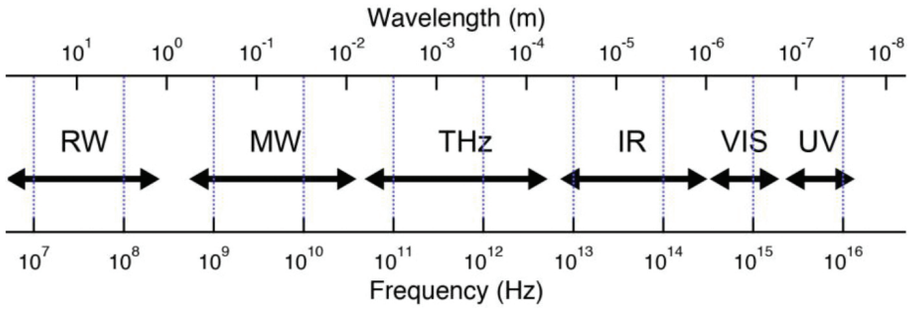


Figure 1. Frequency ranges of electromagnetic waves. RW, MW, THz, IR, VIS, and UV stand for radio waves, microwaves, terahertz, infrared, visible, and ultraviolet, respectively.

To develop active THz devices such as active filters, modulators, and imagers, numerous attempts have been made to modulate THz radiation by external stimuli such as optical, electrical, and thermal stimuli [2–4]. For such purposes, inorganic semiconductor substrates, such as Si [5–8], GaAs [9], and InSb [10], have been widely used since sufficient amounts of free carriers for modulation of THz transmission can easily be obtained by light irradiation (**Figure 2(a)**) or thermal heating. Recently, Yoo et al. reported that depositing a thin layer of organic π-conjugated material, copper phthalocyanine (CuPc) on Si substrate is quite effective to enhance an efficiency of the photo-induced modulation of the THz transmission through it [11–13]. The molecular structure of CuPc is shown in **Figure 2(b)**. They have shown that the THz transmission through CuPc-coated Si substrate decreases under low-power (tens of mW) continuous-wave (CW) laser light irradiation (**Figure 2(c)**) [11]. When only Si substrate was used, or when CuPc was deposited on a quartz substrate instead of on Si, no remarkable modulation was obtained [11]. The authors infer that this is caused by a charge transfer from Si to CuPc. It is impossible to create free charge carriers in CuPc directly via photo-excitation. This is because Frenkel-type tightly bound electron–hole pairs (excitons) are formed, which cannot be dissociated easily due to the strong exciton binding energy typical in organic π-conjugated materials with low dielectric permittivity. Therefore, the interface between organic and inorganic semiconductors should play a crucial role in the modulation mechanism. Free charge carriers should be created in Si by laser light irradiation, and these charge carriers move into thin layer of CuPc. Yoo et al. also showed that optical THz modulation could be induced

http://dx.doi.org/10.5772/64033

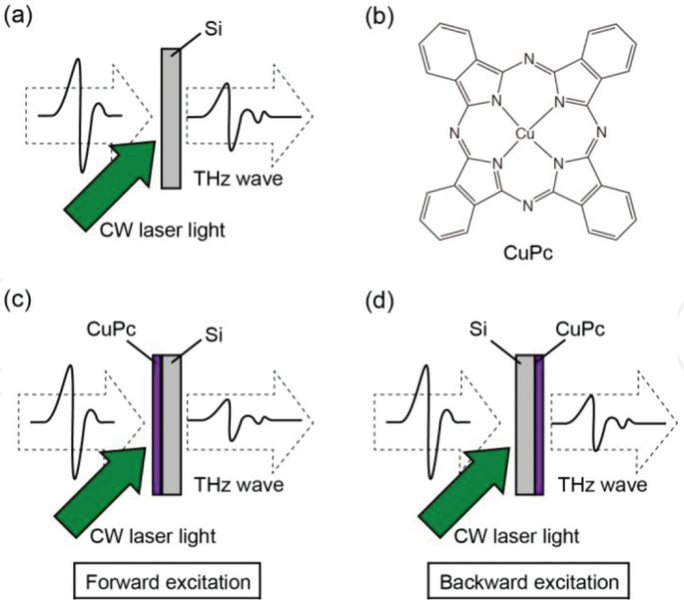


Figure 2. Schematic representation of optical modulation of THz transmission. (a) in Si substrate and (b) molecular structure of CuPc. Efficient optical modulation of THz transmission in Si substrate coated with thin layer of CuPc in (c) forward and (d) backward excitation configurations.

by backward excitation, that is, excitation from the Si substrate (**Figure 2(d)**) [12]. This technique is suitable for materials that show strong absorption at the wavelength of exciting laser light.

Here, we show that the thickness of the organic semiconductor thin film is the crucial parameter for obtaining a high carrier density for metallization and a higher THz transmission modulation [14].

To utilize metamaterials, which show exotic functionality not found in natural materials, is also actively studied for use in developing active THz devices [15–18]. The subwavelength resonant structures such as split-ring resonators (SRRs) can resonantly interact even with magnetic field of electromagnetic waves and give various types of novel functionalities. We also demonstrated that the CuPc/Si system could be used to efficiently control THz resonant responses of SRR array metamaterials that is also fabricated by printing technology [14].

Several groups showed that other types of π-conjugated materials could be used instead of CuPc such as pentacene and C60 [19], poly[2-methoxy-5-(2-ethylhexyloxy)-1,4-phenylenevinylene] (MEH-PPV) [20], various phthalocyanine compounds [21], and 6,13-bis(triisopropylsilylethynyl) pentacene (TIPS-pentacene) [22]. Zhang et al. also succeeded in obtaining highly efficient optical modulation using organometal halide perovskite deposited on Si [23]. Here, we show that various types of organic semiconductors with solution processability can also be utilized for the optical modulation of THz radiation [24]. In this study, the following four soluble organic π-conjugated materials were investigated. Molecular structures of these materials are summarized in **Figure 3**. Two of them were low molecules: a well-known fullerene derivative electron acceptor, [6,6]-phenyl-C61-butyric acid methyl ester (PCBM)

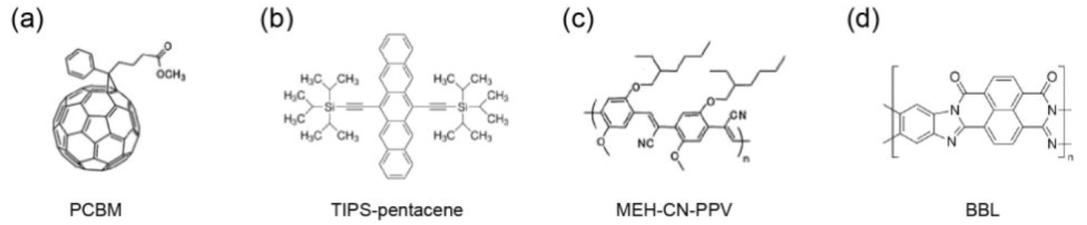


Figure 3. Molecular structures of π-conjugated materials used in this study. (a) [6,6]-phenyl-C61-butyric acid methyl ester (PCBM), (b) 6,13-bis(triisopropylsilylethynyl) pentacene (TIPS-pentacene), (c) poly[5-(2-ethylhexyloxy)-2-methoxycyanoterephthalyliden] (MEH-CN-PPV), and (d) poly(benzimidazobenzophenanthroline) (BBL).

(**Figure 3(a)**) [25–27], and 6,13-bis(triisopropylsilylethynyl) pentacene (TIPS-pentacene) (**Figure 3(b)**), which is extensively studied as an active layer of organic thin-film transistors [28, 29]. The other two materials were π-conjugated polymer materials: n-type semiconductor, poly[5-(2-ethylhexyloxy)-2-methoxycyanoterephthalyliden] (MEH-CN-PPV) (**Figure 3(c)**) [30], and poly(benzimidazobenzophenanthroline) (BBL) (**Figure 3(d)**), which is known as a π-conjugated double-stranded (ladder) polymer with quite a high electron mobility of 0.1 $cm^2 V^{-1} s^{-1}$ [31, 32]. Efficient optical modulation of THz transmission in these solution-processable π-conjugated materials may open the way for printed THz electronics and photonics.

2. Experiment

2.1. Sample preparation

We used a 540-μm-thick, highly resistive Si (>2.0 × 10^4 Ωcm, Optostar Ltd.) that is transparent to THz wave as a substrate. We purchased copper(II) phthalocyanine (β-form powders) from Sigma-Aldrich and used without purification. A thin film of CuPc was deposited by thermal evaporation and subsequently annealed at 250°C to obtain highest modulation, as reported by Yoo et al. [13]. We also used another solution-processable π-conjugated materials, PCBM, TIPS-pentacene, MEH-CN-PPV, and BBL, and these four materials were purchased from Sigma-Aldrich and used without purification [24]. As solvents for solution processes, toluene was used for PCBM and TIPS-pentacene, and chloroform was used for MEH-CN-PPV. To form thin films, spin-coating were used and these films were subsequently thermally annealed at 250°C. BBL thin films were formed using methanesulfonic acid (MSA) as solvent. BBL thin films were spin-coated and immersed in deionized water to remove any remaining MSA solvent following a reported recipe to facilitate aggregation and crystallization [31, 32]. Since BBL thin films easily peel off from the substrate when they are immersed in water, special care has to be taken [24].

We also used printing technology to fabricate SRR array metamaterials. We have utilized a superfine inkjet printer (SIJ printer, SIJTechonology, Inc.) [33–36] to draw a silver SRR array. The sample was subsequently annealed at 240°C. An SRR array with a total area of 5 × 5 mm^2 was fabricated. The dimensions of each SRR meta-atom were designed following

http://dx.doi.org/10.5772/64033

the design of Padilla et al. such that they showed resonant responses in the THz region [16]; therefore, the period (Λ), side length (L), width (W), and gap (G) were made to be 100, 60, 12, and 6 μm, respectively, as shown in **Figure 4(a)**. Such SRRs are known to show electric–magnetic-coupled resonance (ω_0) and half-wave resonance (ω_1) around 1 THz as schematically shown in **Figure 4(b)**.

2.2. THz time-domain spectroscopy measurements

The optical characteristics in the THz range were investigated using typical THz time-domain spectroscopy (THz-TDS) [37–39]. Typical setup and principle of data acquisition are schematically summarized in **Figure 5**. In our setup, photoconductive antennas were used for both generation and coherent detection of THz radiation. The samples were placed in between of two off-axis parabolic mirrors, which are used to collect, collimate, and focus the THz radiation and such that the THz beam was normally incident on the sample surface. For normalization purposes, we also measure reference spectra without placing the samples in the THz beam path as shown in **Figure 5(b)**. A unique feature of the THz-TDS is that it allows for a direct measurement of the transient electric field, so that both amplitude and phase information are obtained simultaneously. Obtained time-domain transient photocurrent responses are Fourier-transformed to evaluate frequency responses as shown in **Figure 5(c)**. We obtain frequency-domain sample response $E_{sam}(\omega)$ and reference $E_{ref}(\omega)$ as follows.

$$E_{sam}(t) \xrightarrow{FT} \left|E_{sam}(\omega)\right| \exp\left\{i\theta_{sam}(\omega)\right\} \tag{1}$$

$$E_{ref}(t) \xrightarrow{FT} \left|E_{ref}(\omega)\right| \exp\left\{i\theta_{ref}(\omega)\right\} \tag{2}$$

By taking a ratio of these frequency-domain responses, transmission coefficient $t(\omega)$ should be evaluated as follows.

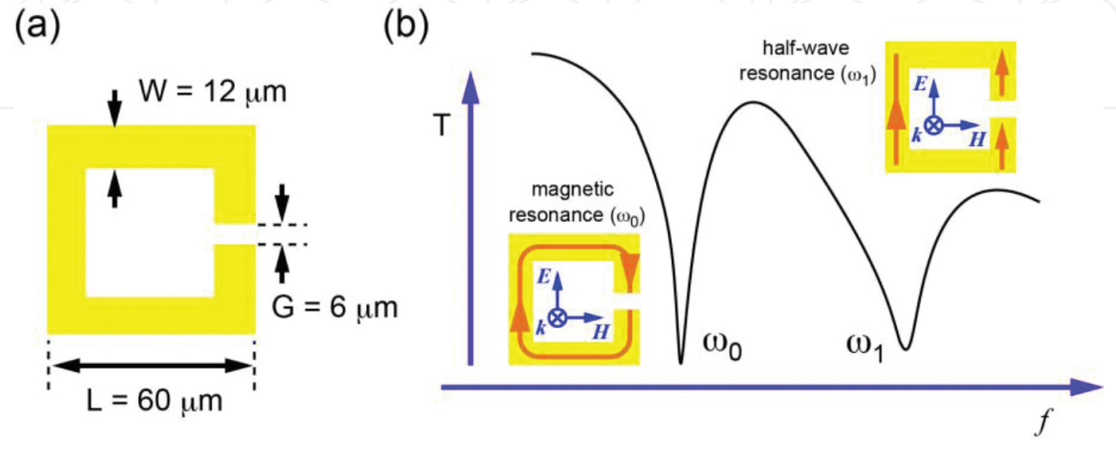


Figure 4. (a) Dimension of each SRR and (b) magnetic resonance and half-wave resonance of SRR array.

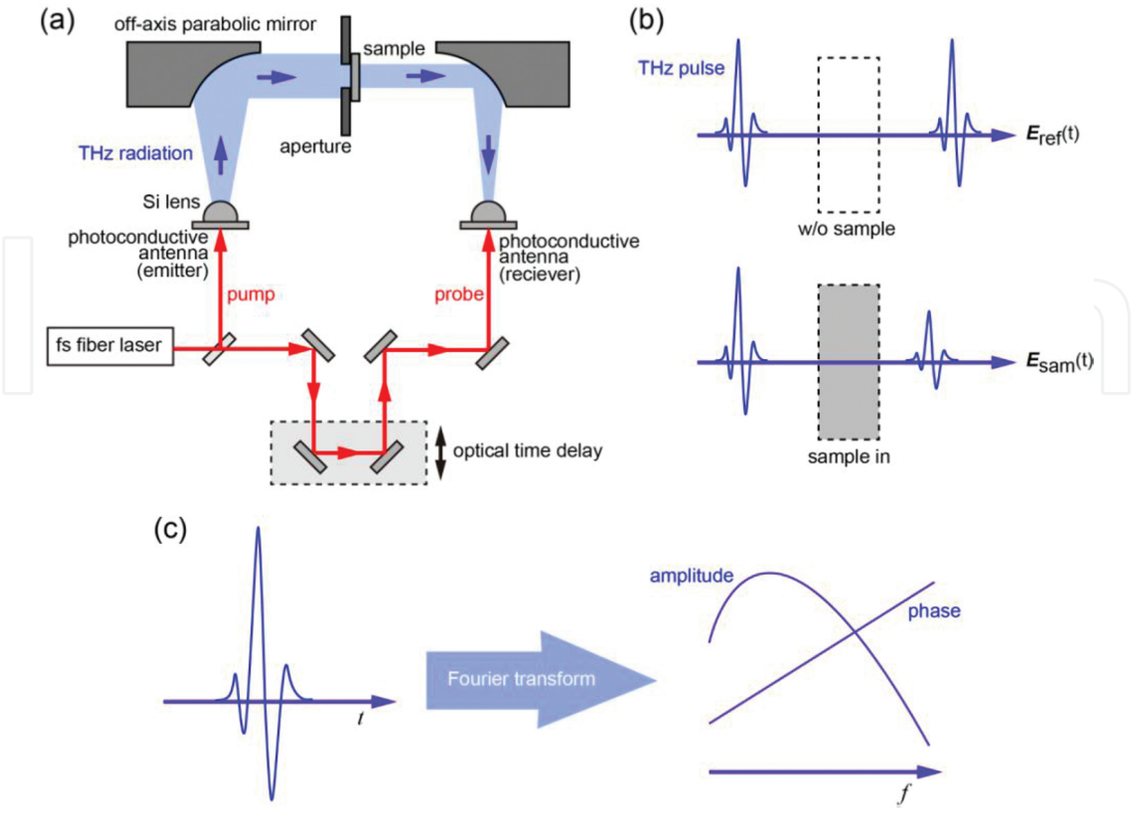


Figure 5. Schematic representation of THz-TDS measurements. (a) Typical setup, (b) time-domain measurements, and (c) retrieving frequency-domain responses by applying Fourier transform to time-domain signal.

$$t(\omega) = \frac{E_{sam}(\omega)}{E_{ref}(\omega)} = \frac{|E_{sam}(\omega)|}{|E_{ref}(\omega)|} \exp\left[i\{\theta_{sam}(\omega) - \theta_{ref}(\omega)\} \right] \tag{3}$$

The transmission coefficient $t(\omega)$ should also be written down with complex refractive indices; therefore, both real (n) and imaginary (κ) refractive indices spectra should be retrieved using amplitude and phase information in experimentally obtained transmission coefficiencies without the need for Kramers–Kronig analysis. We also obtained the complex dielectric constants and complex conductivities from known relations between them and the complex refractive index.

To perform the optical modulation experiment, a 532-nm CW laser (Spectra Physics, Millennia Vs) was used to optically generate free charge carriers in Si. At this wavelength, CuPc and PCBM do not show much absorption; thus, forward excitation configuration was employed, as shown in **Figure 2(c)**. In contrast, TIPS-pentacene, MEH-CN-PPV, and BBL show strong absorption at 532 nm; therefore, backward excitation configuration was used to avoid absorption in π-conjugated materials, as shown in **Figure 2(d)** [24]. A 3-mm-diameter aperture was placed in front of the sample to define the area illuminated by THz radiation.

http://dx.doi.org/10.5772/64033

To quantitatively evaluate the degree of optical modulation of THz transmission, we introduced following modulation factor (MF) of THz transmission:

$$MF = \frac{\int \left|E_{OFF}(\omega)\right|^2 d\omega - \int \left|E_{ON}(\omega)\right|^2 d\omega}{\int \left|E_{OFF}(\omega)\right|^2 d\omega} \quad (4)$$

where $E_{OFF}(\omega)$ and $E_{ON}(\omega)$ are the field amplitudes of the transmitted THz radiation when the CW laser is off and on, respectively. The integration in Eq. (4) was performed over a frequency range from 0.2 to 1.5 THz. A higher MF means a larger drop in THz transmission by CW laser light irradiation [14].

The photo-induced change of the THz responses of SRR array was investigated using the same THz-TDS system. The electric field of the linearly polarized THz radiation is made to be perpendicular to the SRR gap, so that magnetic resonance can be initiated as schematically shown in **Figure 4(b)** [16].

3. Results and discussions

3.1. Efficient optical modulation of THz transmission in Si substrate coated with thin layer of CuPc

In **Figure 6(a)**, the transmitted THz power spectra without laser light irradiation are shown for the bare Si substrate and Si coated with CuPc of different thicknesses of 50, 100, 200, 300, and 500 nm, respectively. There is no significant difference in transmitted power between the bare Si and CuPc-coated Si. In **Figure 6(b)**, the THz transmission spectra of the same samples under laser light irradiation with an intensity of 2.5×10^3 mW/cm^2 are shown. Upon laser light irradiation, the THz transmission decreases to almost zero, especially in CuPc thinner than 200 nm. However, the transmission modulation becomes smaller when the thickness of CuPc is further increased. In **Figure 6(c)**, the MF of the THz transmission is summarized as a function of CuPc film thickness. Without the CuPc film, MF is around 0.54. On the contrary, MF increases drastically to almost unity by depositing a CuPc film thinner than 200 nm. However, MF decreases again with further increasing CuPc thickness and becomes almost the same as without the CuPc film. The charge carrier transfer from Si to CuPc play a crucial role in the THz transmission modulation. Since the absorption coefficient of Si at 530 nm is 7850 cm^{-1} [40], the optical excitation of free charge carriers should occur at the surface (interface) of the Si to a skin depth of micrometers. The bended energy band relationship at the interface drives the free charge carriers to move towards the Si/CuPc interface and transfer into the CuPc layer. When the CuPc layer is thin enough, the charge carrier density increases after being transferred to the CuPc layer and shifts the plasma frequency to a frequency high enough to show metallic characteristics in the THz spectral range. This concentration effect of the transferred free charge carriers in the thin CuPc layer might be the major contribution in the metallization of CuPc, which agrees well with the CuPc thickness dependence of MF shown in **Figure 6(c)**. On the

contrary, when thicker CuPc films were deposited, the CuPc behaves as a dielectric due to the relatively low charge carrier density and therefore becomes more transparent and the MF decreases.

Figure 6(d) shows the transmitted THz power spectra through CuPc-coated Si under different laser light irradiances. The thickness of the CuPc film was 200 nm. With increasing laser light intensity, the THz transmission decreases gradually and drops to approximately zero at 2.5×10^3 mW/cm^2. **Figure 6(e)** shows the normalized transmission spectra under each laser light intensity. Each spectrum is normalized to those with no laser irradiation. The THz transmission modulation is more remarkable at lower frequencies. In **Figure 6(f)**, the MF in Si coated with 200-nm-thick CuPc and bare Si are summarized as a function of laser intensity. The MF is drastically enhanced by the deposition of a 200-nm CuPc film. These results clearly indicate that the THz transmission modulation can be enhanced easily by a simple deposition of a thin CuPc film.

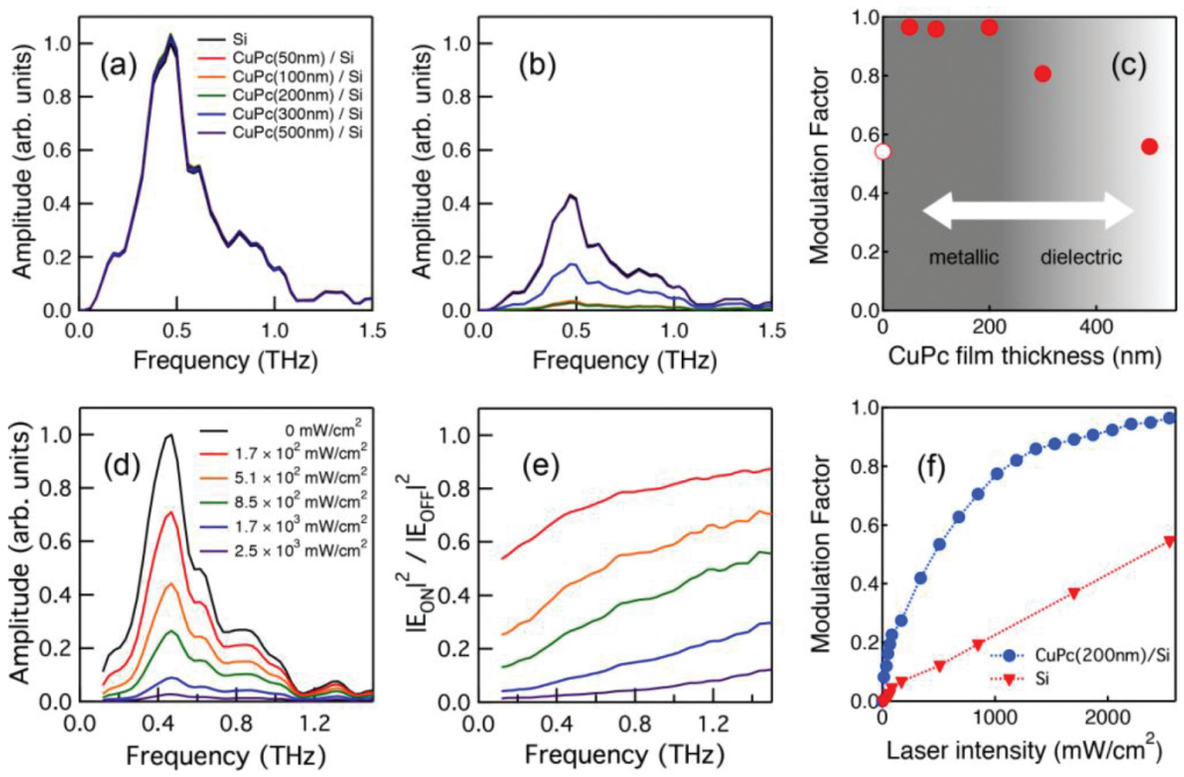


Figure 6. Summary of optical modulation of THz transmission experiment in CuPc-coated Si substrate. THz transmission spectra through a bare Si substrate and Si coated with thin CuPc films of different thicknesses (a) without and (b) with a laser light irradiation of 2.5×10^3 mW/cm^2. (c) CuPc film thickness dependence on the MF for THz transmissions. THz transmission spectra through a 200-nm CuPc film on a Si substrate (d) under different laser light irradiances and (e) those of normalized with THz transmission spectra without laser irradiation. (f) The laser intensity dependence of the MF for THz transmission through a bare Si substrate and Si coated with a 200-nm CuPc film.

In order to investigate further the underlying physical mechanism of the enhanced modulation efficiency of the THz transmission, we compare the dielectric properties of bare Si and CuPc-

http://dx.doi.org/10.5772/64033

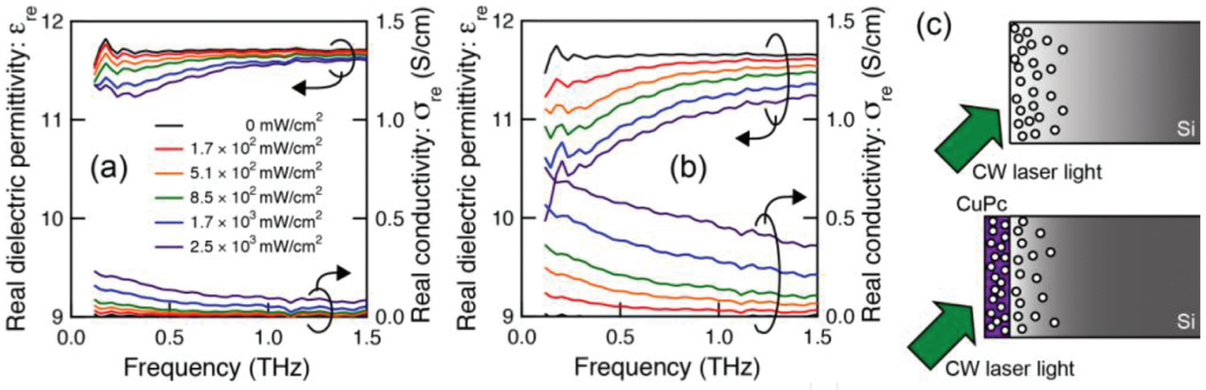


Figure 7. Real dielectric permittivity (ε_{re}) and real conductivity (σ_{re}) spectra under different laser light irradiances of (a) a bare Si substrate and (b) a Si substrate coated with a 200-nm CuPc film analyzed as a composite. (c) Schematic representation of photo-induced charge carrier distribution in a bare Si and a Si substrate coated with a 200-nm CuPc film under laser light irradiation.

coated Si under different laser light irradiation conditions. **Figure 7(a)** shows real dielectric permittivity (ε_{re}) and the real conductivity (σ_{re}) spectra of a bare Si substrate, and **Figure 7(b)** shows corresponding spectra for a 200-nm CuPc film on a Si substrate under different laser light irradiances. We have analyzed CuPc-coated Si as a single-layer composite material, because we think the THz dielectric characteristics of CuPc/Si two-layer system cannot be analyzed separately. In order to analyze them separately, we first need to have dielectric characteristics of bare Si with separate experiment. However, as schematically shown in **Figure 7(c)**, when Si is coated with thin layer of CuPc, the density of charge carrier in the Si upon CW laser light irradiation condition should be different from that of bare Si. Therefore, the THz response of the Si side of CuPc-coated Si should be different from that of the bare Si substrate. This is the reason why we have analyzed CuPc-coated Si as a single-layer composite material [14].

Without laser irradiation, the dielectric response shows almost no dispersion and almost the same value with and without the CuPc film as shown in **Figure 7(a)** and **(b)**. However, with increasing laser light intensity, the real dielectric permittivity decreases especially at lower frequencies, which can be attributed to a Drude-like metallic response. This may explain why higher modulation was obtained for lower frequencies as shown in **Figure 6(e)** [14]. Although the thickness of CuPc is <0.5% of that of Si, the change in the dielectric response by CW laser light irradiation is remarkable in CuPc-coated Si. This implies that the contribution from thin CuPc layer to the dielectric property is quite large; therefore, the change in the dielectric permittivity of the CuPc layer should be much larger than it appeared. It may be reasonable to expect that the permittivity drops to negative values, like in a Drude-like response. The change in real conductivity by CW laser light irradiation is also remarkable in CuPc-coated Si, and the real conductivity in CuPc layer should also be much higher than it appeared under laser light irradiation. The significant increase in conductivity by CW laser light irradiation also supports that CuPc-coated Si becomes more conductive [14].

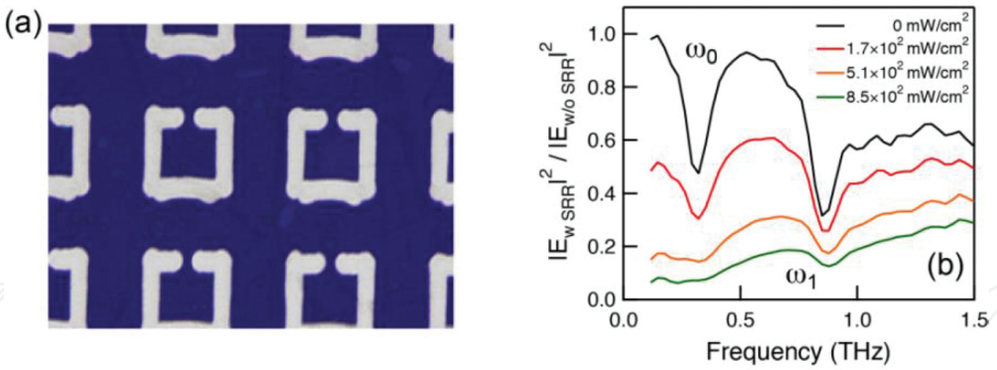


Figure 8. (a) Laser microscope image of the fabricated Ag SRR array on a 200-nm CuPc film on a Si substrate. (b) Normalized THz transmission spectra under different laser light irradiances through the SRR array fabricated on a 200-nm CuPc film on a Si substrate.

3.2. Efficient optical modulation of THz resonant responses in printed SRR array on Si substrate coated with thin layer of CuPc

We have applied efficient optical modulation of THz transmission through the Si substrate coated with thin film of CuPc to the optical modulation of SRR metamaterial responses. We fabricated SRR array on CuPc-coated Si by using superfine inkjet printer. **Figure 8(a)** shows a laser microscope image of the fabricated silver SRR array. **Figure 8(b)** shows the normalized THz transmission spectra of it under different laser light irradiances. When the laser light is off, sharp transmission dips induced by resonant interaction with the SRRs can be recognized. The dip in transmission at the lower (ω_0 ~0.32 THz) and higher (ω_1 ~0.85 THz) frequencies could be attributed to the electric–magnetic-coupled resonance and the half-wave resonance, respectively (**Figure 4(b)**) [16]. As the laser light intensity is increased, the transmission drops in all frequencies of interest and almost no features can be recognized at higher laser light intensities. The efficient metallization in CuPc-coated Si by CW laser light irradiation is enough to short the capacitive gap of the SRR and erase its resonant effect [14]. For more efficient modulation at particular frequencies, CuPc should be partially coated only on the capacitive gap of the SRR, for example.

3.3. Efficient optical modulation of THz transmission in Si substrate coated with thin layer of solution-processable π-conjugated materials

We have further investigated optical modulation characteristics of THz transmission in Si substrate coated with thin layer of solution-processable π-conjugated materials. In **Figure 9**, MF of the THz transmission through Si substrates coated with four different π-conjugated materials, PCBM, TIPS-pentacene, MEH-CN-PPV, and BBL, are summarized as a function of laser intensity. Those of CuPc are also shown for comparison. Since the modulation efficiency is not the same for different ways of excitations (forward or backward excitations) [12], in **Figure 9(a)** and **(b)**, we summarize our data separately for forward and backward excitations, respectively. In all the samples, a significant increase in MF was obtained upon illumination with the CW laser light. Among these, PCBM and TIPS-pentacene are more efficient than CuPc;

http://dx.doi.org/10.5772/64033

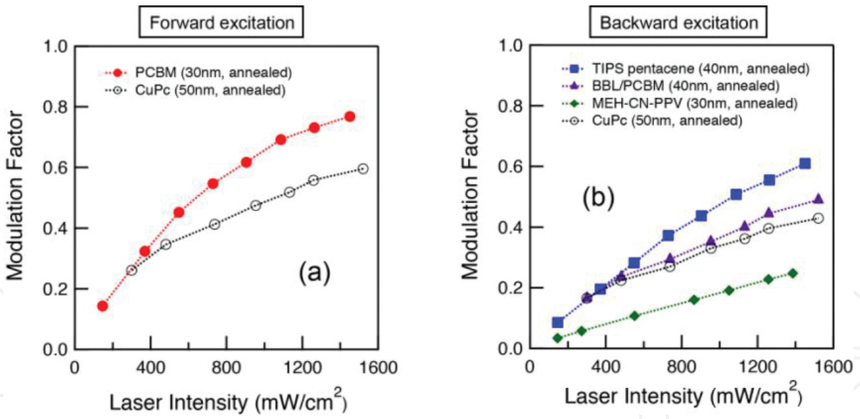


Figure 9. Summary of the laser intensity dependence of the MF of THz transmission in the (a) PCBM and CuPc with forward excitation and (b) TIPS-pentacene, BBL/PCBM, MEH-CN-PPV, and CuPc with backward excitation.

therefore, PCBM and TIPS-pentacene are more useful not only from the viewpoint of the fabrication process but also modulation efficiency. In these two materials, it was also found that thermal annealing was effective in further increasing MF (data are not shown).

4. Conclusions

In conclusions, we have analyzed the optical modulation characteristics of THz transmission in Si substrate coated with organic π-conjugated materials under various laser light irradiation conditions using THz-TDS. The charge carrier transfer from Si to organic π-conjugated materials plays crucial role for the photo-induced metallization of Si coated with organic π-conjugated materials, and it was shown that the thickness of the organic layer is a critical parameter to realize higher modulation efficiency. We have also fabricated SRR array metamaterial by using superfine inkjet printer on CuPc-coated Si and demonstrated efficient modulation of the resonant responses of SRR by laser light irradiation. We have also investigated optical modulation of THz transmission of Si coated with four types of π-conjugated materials: two low molecules PCBM and TIPS-pentacene, and two π-conjugated polymer materials MEH-CN-PPV and BBL. Among these materials, PCBM and TIPS-pentacene showed higher modulation efficiencies, even higher than that of CuPc. Utilizing these solution processable π-conjugated materials, various types of THz materials and devices could be fabricated by printing technologies.

Acknowledgements

This work is dedicated to Professor Masanori Hangyo, who jointly conceived the idea and led our team, and passed away on 25 October 2014. This work has been partially supported by a Grant-in-Aid for Scientific Research on Innovative Areas (Nos. 22109001 and 25109709) from

the Ministry of Education, Culture, Sports, Science, and Technology Japan (MEXT), and a Grant-in-Aid for Scientific Research, KAKENHI, for Scientific Research (B), No. 25286063, from the Japan Society for the Promotion of Science (JSPS) and by the joint research project of the Institute of Laser Engineering, Osaka University (No. 2015B1-17). The authors acknowledge graduate students, Mr. Ryosuke Takagi, Mr. Yuto Inose, Mr. Shota Kuromiya, and Mr. Hiroki Mori, who contributed to this work.

Author details

Tatsunosuke Matsui[1,2*], Keisuke Takano[3], Makoto Nakajima[3] and Masanori Hangyo[3]

*Address all correspondence to: matsui@elec.mie-u.ac.jp

1 Department of Electrical and Electronic Engineering, Graduate School of Engineering, Mie University, Tsu, Japan

2 The Center of Ultimate Technology on Nano-Electronics, Mie University, Tsu, Japan

3 Institute of Laser Engineering, Osaka University, Suita, Osaka, Japan

References

[1] Tonouchi M. Cutting-edge terahertz technology. Nature Photonics. 2007;1:97–105. doi: 10.1038/nphoton.2007.3

[2] Hangyo M. Development and future prospects of terahertz technology. Japanese Journal of Applied Physics. 2015;54:120101-1–120101-16. doi:10.7567/JJAP.54.120101

[3] Rahm M, Li JS, Padilla WJ. THz wave modulators: a brief review on different modulation techniques. Journal of Infrared, Millimeter, and Terahertz Waves. 2013;34:1–27. doi:10.1007/s10762-012-9946-2

[4] Azad AK, O'Hara JF, Singh R, Chen HT, Taylor AJ. A review of terahertz plasmonics in subwavelength holes on conducting films. IEEE Journal of Selected Topics in Quantum Electronics. 2013;19:8400416. doi:10.1109/JSTQE.2012.2208181

[5] Kitoh Y, Yamashita M, Nagashima T, Hangyo M. Terahertz beam profiler using optical transmission modulation in silicon. Japanese Journal of Applied Physics. 2001;40:L1113–L1115. doi:10.1143/JJAP.40.L1113

[6] Rivas JG, Bolivar PH, Kurz H. Thermal switching of the enhanced transmission of terahertz radiation through subwavelength apertures. Optics Letters. 2004;29:1680–1682. doi:10.1364/OL.29.001680

[7] Hendry E, Garcia-Vidal FJ, Martin-Moreno L, Rivas JG, Bonn M, Hibbins AP, Lockyear MJ. Optical control over surface-plasmon-polariton-assisted THz transmission through a slit aperture. Physical Review Letters. 2008;100:123901-1–123901-4. doi:10.1103/PhysRevLett.100.123901

[8] Okada T, Tanaka K. Photo-designed terahertz devices. Scientific Reports. 2011;1:121-1–121-5. doi:10.1038/srep00121

[9] Chen Q, Jiang Z, Xu GX, Zhang XC. Near-field terahertz imaging with a dynamic aperture. Optics Letters. 2000;25:1122–1124. doi:10.1364/OL.25.001122

[10] Rivas JG, Janke C, Bolivar PH, Kurz H. Transmission of THz radiation through InSb gratings of subwavelength apertures. Optics Express. 2005;13:847–859. doi:10.1364/OPEX.13.000847

[11] Yoo HK, Kang C, Yoon Y, Lee H, Lee JW, Lee K, Kee CS. Organic conjugated material-based broadband terahertz wave modulators. Applied Physics Letters. 2011;99:061108-1–061108-3. doi:10.1063/1.3626591

[12] Yoo HK, Kang C, Lee JW, Yoon Y, Lee H, Lee K, Kee CS. Transmittances of terahertz pulses through organic copper phthalocyanine films on Si under optical carrier excitation. Applied Physics Express. 2012;5:072402-1–072402-3. doi:10.1143/APEX.5.072402

[13] Yoo HK, Lee SG, Kang C, Kee CS, Lee JW. Terahertz modulation on angle-dependent photoexcitation in organic inorganic hybrid structures. Applied Physics Letters. 2013;103:151116-1–151116-3. doi:10.1063/1.4825170

[14] Matsui T, Takagi R, Takano K, Hangyo M. Mechanism of optical terahertz-transmission modulation in an organic/inorganic semiconductor interface and its application to active metamaterials. Optics Letters. 2013;38:4632–4635. doi:10.1364/OL.38.004632

[15] Yen TJ, Padilla WJ, Fang N, Vier DC, Smith DR, Pendry JB, Basov DN, Zhang X. Terahertz magnetic response from artificial materials. Science. 2004;303:1494–1496. doi:10.1126/science.1094025

[16] Padilla WJ, Taylor AJ, Highstrete C, Lee M, Averitt RD. Dynamical electric and magnetic metamaterial response at terahertz frequencies. Physical Review Letters. 2006;96:107401-1–107401-4. doi:10.1103/PhysRevLett.96.107401

[17] Chen HT, Padilla WJ, Zide JMO, Gossard AC, Taylor AJ, Averitt RD. Active terahertz metamaterial devices. Nature. 2006;444:597–600. doi:10.1038/nature05343

[18] Chen HT, O'Hara JF, Azad AK, Taylor AJ, Averitt RD, Shrekenhamer DB, Padilla WJ. Experimental demonstration of frequency-agile terahertz metamaterials. Nature Photonics. 2008;2:295–298. doi:10.1038/nphoton.2008.52

[19] Yoo HK, Yoon Y, Lee K, Kang C, Kee CS, Hwang IW, Lee JW. Highly efficient terahertz wave modulators by photo-excitation of organics/silicon bilayers. Applied Physics Letters. 2014;105:011115-1–011115-5. doi:10.1063/1.4887376

[20] Zhang B, He T, Shen J, Hou Y, Hu Y, Zang M, Chen T, Feng S, Teng F, Qin L. Conjugated polymer-based broadband terahertz wave modulator. Optics Letters. 2014;39:6110–6113. doi:10.1364/OL.39.006110

[21] He T, Zhang B, Shen J, Zang M, Chen T, Hu Y, Hou Y. High-efficiency THz modulator based on phthalocyanine-compound organic films. Applied Physics Letters. 2015;106:053303-1–053303-5. doi:10.1063/1.4907651

[22] Park JM, Sohn IB, Kang C, Kee CS, Hwang IW, Yoo HK, Lee JW. Terahertz modulation using TIPS-pentacene thin films deposited on patterned silicon substrates. Optics Communications. 2016;359:349–352. doi:10.1016/j.optcom.2015.10.008

[23] Zhang B, Lv L, He T, Chen T, Zang M, Zhong L, Wang X, Shen J, Hou Y. Active terahertz device based on optically controlled organometal halide perovskite. Applied Physics Letters. 2015;107:093301-1–093301-4. doi:10.1063/1.4930164

[24] Matsui T, Mori H, Inose Y, Kuromiya S, Takano K, Nakajima M, Hangyo M. Efficient optical terahertz-transmission modulation in solution-processable organic semiconductor thin films on silicon substrate. Japanese Journal of Applied Physics. 2016;55:03DC12-1–03DC12-4. doi:10.7567/JJAP.55.03DC12

[25] Hummelen JC, Knight BW, LePeq F, Wudl F, Yao J, Wilkins CL. Preparation and characterization of fulleroid and methanofullerene derivatives. Journal of Organic Chemistry. 1995;60:532–538. doi:10.1021/jo00108a012

[26] Rispens MT, Meetsma A, Rittberger Brabec RCJ, Sariciftci NS, Hummelen JC. Influence of the solvent on the crystal structure of PCBM and the efficiency of MDMO-PPV:PCBM 'plastic' solar cells. Chemical Communications. 2003;17:2116–2118. doi:10.1039/B305988J

[27] Anthopoulos TD, de Leeuw DM, Cantatore E, Setayesh S, Meijer EJ, Tanase C, Hummelen JC, Blom PWM. Organic complementary-like inverters employing methanofullerene-based ambipolar field-effect transistors. Applied Physics Letters. 2004;85:4205–4207. doi:10.1063/1.1812577

[28] Anthony JE, Brooks JS, Eaton DL, Parkin SR. Functionalized Pentacene: improved electronic properties from control of solid-state order. Journal of American Chemical Society. 2001;123:9482–9483. doi:10.1021/ja0162459

[29] Sheraw CD, Jackson TN, Eaton DL, Anthony JE. Functionalized Pentacene active layer organic thin-film transistors. Advanced Materials. 2003;15:2009–2011. doi:10.1002/adma.200305393

[30] Ruderer MA, Wang C, Schaible E, Hexemer A, Xu T, Muller-Buschbaum P. Morphology and optical properties of P3HT:MEH-CN-PPV blend films. Macromolecules. 2013;46:4491–4501. doi:10.1021/ma4006999

[31] Babel A, Jenekhe SA. High electron mobility in ladder polymer field-effect transistors. Journal of American Chemical Society. 2003;125:13656–13657. doi:10.1021/ja0371810

[32] Alam MM, Jenekhe SA. Efficient solar cells from layered nanostructures of donor and acceptor conjugated polymers. Chemistry of Materials. 2004;16:4647–4656. doi:10.1021/cm0497069

[33] Murata K, Matumoto J, Tezuka A, Matsuba Y, Yokoyama H. Super-fine ink-jet printing: toward the minimal manufacturing system. Microsystem Technologies. 2005;12:2–7. doi:10.1007/s00542-005-0023-9

[34] Murata K, Masuda K. Super inkjet printer technology and its properties. E-Print Printable Electronics. 2011;1:108–111.

[35] Takano K, Kawabata T, Hsieh CF, Akiyama K, Miyamaru F, Abe Y, Tokuda Y, Pan RP, Pan CL, Hangyo M. Fabrication of terahertz planar metamaterials using the super-fine ink-jet printer. Applied Physics Express. 2010;3:016701-1–016701-3. doi:10.1143/APEX.3.016701

[36] Takano K, Chiyoda Y, Nishida T, Miyamaru F, Kawabata T, Sasaki H, Takeda MW, Hangyo M. Optical switching of terahertz radiation from meta-atom-loaded photoconductive antennas. Applied Physics Letters. 2011;99:161114-1–161114-3. doi:10.1063/1.3654156

[37] Grischkowsky D, Keiding S, van Exter M, Fattinger C. Far-infrared time-domain spectroscopy with terahertz beams of dielectrics and semiconductors. Journal of Optical Society of America B. 1990;7:2006–2015. doi:10.1364/JOSAB.7.002006

[38] Hangyo M, Tani M, Nagashima T. Terahertz time-domain spectroscopy of solids: a review. International Journal of Infrared and Millimeter Waves. 2005;26:1661–1690. doi:10.1007/s10762-005-0288-1

[39] Lloyd-Hughes J, Jeon TI. A review of the terahertz conductivity of bulk and nanomaterials. International Journal of Infrared and Millimeter Waves. 2012;33:871–925. doi:10.1007/s10762-012-9905-y

[40] Nakato Y, Shioji M, Tsubomura H. Photovoltage and stability of an n-type silicon semiconductor coated with metal or metal-free phthalocyanine thin films in aqueous redox solutions. Journal of Physical Chemistry. 1981;85:1670–1672. doi:10.1021/j150612a014

IntechOpen

IntechOpen